

Active particles in viscosity gradients

Charu Datt and Gwynn J. Elfring*

*Department of Mechanical Engineering and Institute of Applied Mathematics,
University of British Columbia, Vancouver, BC, V6T 1Z4, Canada*

(Dated: April 19, 2022)

Microswimmers in nature often experience spatial gradients of viscosity. In this work we develop theoretical results for the dynamics of active particles, biological or otherwise, swimming through viscosity gradients. We model the active particles (or swimmers) using the squirmer model, and show how the effects of viscosity gradients depend on the swimming gait of the swimmers and how viscosity gradients lead to viscotaxis for squirmers. We also show how such gradients in viscosity may be used to sort swimmers based on their swimming style.

Cells often swim in environments, such as biofilms and mucus layers, that have spatial gradients of viscosity [1, 2]. Much like the effect of other gradients, such as light (leading to phototaxis [3]), chemical stimuli (chemotaxis [4]), magnetic fields (magnetotaxis [5]), temperature (thermotaxis [6]), or gravitational potential (gravitaxis [7]), gradients of viscosity can lead to viscotaxis in microswimmers. Bacteria like *Leptospira* and *Spiroplasma* are known to move up the viscosity gradients (positive viscotaxis) [8, 9], whereas *Escherichia coli* demonstrates negative viscotaxis [10]. It is suggested that viscotaxis plays an adaptive role in microorganisms; it prevents them from being stuck in regions where they are poor swimmers [8–10]. This migration across regions of different viscosity affects organisms’ population distribution, and possibly their virulence [11]. The aggregation of microswimmers in specific regions of viscosity may also be used for sorting of cells [12].

Recent works have investigated the effect of viscosity gradients in fluids on the motion of both passive and active (swimming) particles. The work of Laumann and Zimmermann [13] has shown that viscosity gradients can be used to sort soft passive particles in microflows using the phenomenon of cross-streamline migration. Openheimer *et al.* [14] considered the dynamics of a hot particle in a fluid where variations in viscosity are due to the temperature difference between the particle and its surroundings. In terms of active particles, the works of Liebchen *et al.* [15] and Eastham and Shoele [16] have investigated the motion of model swimmers as they move through gradients of viscosity in an otherwise Newtonian fluid. Liebchen *et al.* [15] studied the physical mechanism of viscotaxis, using assemblies of one, two and three spheres with effective propulsion forces as model swimmers, and showed how viscotaxis can emerge from a mismatch of viscous forces on different parts of the swimmer, thereby demonstrating the possibility of both positive and negative viscotaxis i.e. motion towards or away from regions of higher viscosity, respectively. In particular, they proved that, for these model swimmers, uniaxial swimmers do not display viscotaxis. Eastham and Shoele [16] studied an adaptation of a common model microswimmer—the squirmer [17–19]—as it moves through

fluids in which viscosity is a function of the concentration of nutrients. They find that the coupling between viscosity and nutrient concentration can lead to qualitative differences in the swimming motion compared to fluids with constant viscosity. In fact, they find that swimming gaits that do not lead to net motion in fluids with constant viscosity can lead to swimming in fluids with a nutrient-concentration-dependent viscosity. Similar conclusions were also previously noted for squirming motions in shear-thinning fluids [20].

In this work, we study viscotaxis using the classical spherical squirmer model [17–19]. Squirmers can be used to model different types of swimmers, from biological micro-organisms to diffusiophoretic Janus particles, within the same theoretical framework, and have been used in understanding swimming at small scales in both Newtonian (e.g., see [19] and references within) and non-Newtonian fluids (e.g., [20–25]). The squirmer model allows us to study the response of different classes of microswimmers, namely, pushers, pullers and neutral swimmers, to spatial gradients in viscosity. Notably we find that, in contrast to the results in Liebchen *et al.* [15], these uniaxial swimmers all display (negative) viscotaxis. We also find that the three types of swimmers behave differently in viscosity gradients, and discuss how their different swimming dynamics can be used to sort them based on their swimming style. In the following, we first present the theoretical formulation of the problem, followed by results and discussion.

In the squirmer model a microswimmer is represented as a sphere with a prescribed surface velocity [17] that approximates the detailed propulsion mechanism of the swimmer [17]. We consider axisymmetric squirmers with steady tangential surface velocities $\mathbf{u}^S = u^S \mathbf{e}_\phi$, where $u^S = \sum_{l=1}^{\infty} B_l V_l(\phi)$, and $V_l(\phi) = -2P_l^1(\cos \phi) / (l(l+1))$ with P_l^1 being the associated Legendre function of the first kind and ϕ the polar angle measured from the axis of symmetry of the swimmer [17, 18]. The orientation of the swimmer, along the axis of symmetry is denoted by the unit vector \mathbf{e} (equivalent to the outward normal at $\phi = 0$). The coefficients B_l are called the squirming modes. In Newtonian fluids with constant viscosity, the propulsion velocity of the

squirmers is due to just the first mode B_1 , whereas B_2 gives the strongest contribution to the flow far from the swimmer [18, 26]. With no lack of generality we take $B_1 \geq 0$. For swimmers that generate thrust from the front, the puller type (like *Chlamydomonas*), the ratio $\alpha = B_2/B_1$ is greater than zero, and for those that generate thrust from the rear (like *Escherichia coli*), $\alpha < 0$. Swimmers in which the thrust and drag centres coincide are modelled with $\alpha = 0$ and are called neutral squirmers. Pak and Lauga [27] provide a detailed description of general, non-axisymmetric, squirming modes. We note that a swimming gait, and thus the surface velocities of a squirmer, may be affected by changes in viscosity, but here we assume it remains fixed.

We consider Newtonian fluids with spatial gradients of viscosity that may arise, for example, due to temperature or due to gradients of concentration of solute. To make theoretical progress, we consider only small variations in viscosity, representing the viscosity field as $\eta(\mathbf{x}) = \eta_0 + \varepsilon\eta_1(\mathbf{x})$, where $\varepsilon \ll 1$ is a small dimensionless parameter representing the characteristic magnitude of the change in viscosity $\Delta\eta/\eta_0$. The small viscosity variations, of $\mathcal{O}(\varepsilon)$, allow us to obtain the first effects of viscosity gradients on the motion of the swimmer with the relative ease by utilizing a regular perturbation expansion in ε .

We primarily consider linear viscosity fields with slope η_0/L (in the \mathbf{e}_x direction for example) so that

$$\nabla\eta = \frac{\eta_0}{L}\mathbf{e}_x. \quad (1)$$

Provided the length L is much larger than the size of the swimmer of radius a such that $\varepsilon = a/L \ll 1$, the viscosity varies only weakly in the vicinity of the particle. In this case $\eta_1 = \eta_0(x - x_0)/a$, and η_0 occurs at an arbitrary point x_0 in the fluid.

We neglect any fluid and solid body inertia, and study microswimmers at zero Reynolds number. In the absence of inertia, the velocity of an active (or passive) particle in a fluid of arbitrary rheology may be written as

$$\mathbf{U} = \hat{\mathbf{R}}_{FU}^{-1} \cdot [\mathbf{F}_{ext} + \mathbf{F}_S + \mathbf{F}_{NN}], \quad (2)$$

where $\mathbf{U} = [\mathbf{U} \ \boldsymbol{\Omega}]^\top$ is a six-dimensional vector comprising of rigid-body translational and rotational velocities whereas $\mathbf{F} = [\mathbf{F} \ \mathbf{L}]^\top$ represents force and torque. The expression (2) can be easily derived using the reciprocal theorem of low Reynolds number flows and its formulation as described in [28, 29]. For freely swimming density matched bodies the external force $\mathbf{F}_{ext} = \mathbf{0}$.

The term

$$\mathbf{F}_S = \int_{\partial\mathcal{B}} \mathbf{u}^S \cdot (\mathbf{n} \cdot \hat{\mathbf{T}}_U) dS \quad (3)$$

represents the propulsive force (or swim force [30]) due to any surface deformation or activity \mathbf{u}^S of the particle

in a Newtonian fluid of *uniform* viscosity η_0 . Here $\partial\mathcal{B}$ represents the surface of the particle.

The ‘non-Newtonian’ contribution, or more precisely the contribution due to a deviation from a Newtonian fluid with uniform viscosity, is given by

$$\mathbf{F}_{NN} = - \int_{\mathcal{V}} \boldsymbol{\tau}_{NN} : \hat{\mathbf{E}}_U dV. \quad (4)$$

This term represents the extra force/torque on the particle due to the extra deviatoric stress $\boldsymbol{\tau}_{NN}$ in the fluid volume \mathcal{V} in which the particle is immersed. The total deviatoric stress in the fluid is $\boldsymbol{\tau} = \eta_0\dot{\boldsymbol{\gamma}} + \boldsymbol{\tau}_{NN}$ and so in our case $\boldsymbol{\tau}_{NN} = \varepsilon\eta_1\dot{\boldsymbol{\gamma}}$.

Finally, the hat quantities are linear operators from the resistance/mobility problem of a body of the same shape in a Newtonian fluid of uniform viscosity η_0 : $\hat{\boldsymbol{\gamma}}/2 = \hat{\mathbf{E}}_U \cdot \hat{\mathbf{U}}$, $\hat{\boldsymbol{\sigma}} = \hat{\mathbf{T}}_U \cdot \hat{\mathbf{U}}$, $\hat{\mathbf{F}} = -\hat{\mathbf{R}}_{FU} \cdot \hat{\mathbf{U}}$. For the present case of spherical squirmers, the resistance/mobility problem is the rigid-body motion of a single sphere in an unbounded and otherwise quiescent Newtonian fluid, and therefore $\hat{\mathbf{E}}_U$, $\hat{\mathbf{T}}_U$ and $\hat{\mathbf{R}}_{FU}$ are well known.

The extra stress $\boldsymbol{\tau}_{NN}$ requires resolution of the flow field generated by the swimmer in a fluid with a non-uniform viscosity. This task can be made simpler by considering small deviations from a uniform viscosity $\varepsilon \ll 1$ and thus constructing $\boldsymbol{\tau}_{NN}$ asymptotically. To study the effect of small viscosity variations, quantified by ε , we expand flow quantities in a regular perturbation expansion of ε , e.g., $\{\mathbf{u}, p, \boldsymbol{\tau}\} = \{\mathbf{u}_0, p_0, \boldsymbol{\tau}_0\} + \varepsilon\{\mathbf{u}_1, p_1, \boldsymbol{\tau}_1\} + \varepsilon^2\{\mathbf{u}_2, p_2, \boldsymbol{\tau}_2\} + \dots$, where $\{\mathbf{u}_0, p_0, \boldsymbol{\tau}_0\}$ are the velocity, pressure and deviatoric stress solution to Stokes equations for Newtonian fluids with uniform viscosity η_0 , since at the leading order, $\boldsymbol{\tau}_0 = \eta_0\dot{\boldsymbol{\gamma}}_0$. At $\mathcal{O}(\varepsilon)$, $\boldsymbol{\tau}_1 = \eta_0\dot{\boldsymbol{\gamma}}_1 + \eta_1(\mathbf{x})\dot{\boldsymbol{\gamma}}_0$, so that, $\boldsymbol{\tau}_{NN,1} = \eta_1(\mathbf{x})\dot{\boldsymbol{\gamma}}_0$. The extra force and torque on the particle from (4) then take the form

$$\mathbf{F}_{NN} = \varepsilon \int_{\mathcal{V}} \eta_1(\mathbf{x}) \dot{\boldsymbol{\gamma}}_0 : \hat{\mathbf{E}}_U dV + \mathcal{O}(\varepsilon^2), \quad (5)$$

$$\mathbf{L}_{NN} = \varepsilon \int_{\mathcal{V}} \eta_1(\mathbf{x}) \dot{\boldsymbol{\gamma}}_0 : \hat{\mathbf{E}}_{\boldsymbol{\Omega}} dV + \mathcal{O}(\varepsilon^2). \quad (6)$$

We consider corrections up to $\mathcal{O}(\varepsilon)$ in this work.

Note that the expansion is valid provided that $\eta_1/\eta_0 \sim \mathcal{O}(1)$, and this is in principle not true for $r \sim \mathcal{O}(1/\varepsilon)$. However, for a squirmer in linear or radial viscosity variations the far field contribution, when $r \sim \mathcal{O}(1/\varepsilon)$, is $\mathcal{O}(\varepsilon^2)$ for the extra force and $\mathcal{O}(\varepsilon^3)$ for the extra torque and can therefore be neglected as we consider corrections to Newtonian-uniform-viscosity motion up to only $\mathcal{O}(\varepsilon)$. Now, because the velocity field due to motion of a passive sphere decays slower than that of a squirmer, in principle, the far-field would contribute. However, in linear viscosity profiles, the far-field contribution to the integrals at $\mathcal{O}(1)$ is identically zero (due to symmetry).

Passive particles. We first study the motion of a passive sphere in viscosity gradients, in order to build intuition on the influence of viscosity variations on hydrodynamic drag, and then study the motion of squirmers in these gradients.

The hydrodynamic force \mathbf{F} and torque \mathbf{L} on a rigid sphere of radius a moving with a velocity \mathbf{U} and rotating with an angular velocity $\mathbf{\Omega}$ in a linear viscosity field (1), is found to be, up to $\mathcal{O}(\varepsilon)$,

$$\mathbf{F} = -6\pi a\eta_0 \mathbf{U} + 2\pi a^3 \nabla\eta \times \mathbf{\Omega}, \quad (7)$$

$$\mathbf{L} = -8\pi\eta_0 a^3 \mathbf{\Omega} - 2\pi a^3 \nabla\eta \times \mathbf{U}. \quad (8)$$

It should be noted that the gradient in viscosity couples the force with the sphere's angular velocity, and the torque with the translational velocity; these couplings are absent for a sphere in a Newtonian fluid with uniform viscosity. The coupling is symmetric, which may be proved by the reciprocal theorem as shown by Oppenheimer *et al.* [14], with resistance $\mathbf{R}_{F\Omega} = \mathbf{R}_{LU}^\top = -2\pi a^3 \nabla\eta \times \mathbf{I}$.

Oppenheimer *et al.* [14] studied the case of viscosity gradients induced by a hot particle in a viscous fluid. In this instance the viscosity field may be taken to be

$$\eta = \eta_0 \left(1 - \varepsilon \frac{a}{r}\right), \quad (9)$$

where here $\varepsilon = \Delta\eta/\eta_0$ and r is the distance from the particle of radius a . As a consistency check we reproduce their results using equations (5) and (6), i.e., $\mathbf{F} = -6\pi\eta_0 a \left(1 - \frac{5\varepsilon}{12}\right) \mathbf{U}$, $\mathbf{L} = -8\pi\eta_0 a^3 \left(1 - \frac{3\varepsilon}{4}\right) \mathbf{\Omega}$. It should be noted that in this case the translational and rotational motion are not coupled—because of the symmetry of the gradient—and both the drag and the torque are lower than those for the case of constant viscosity η_0 .

Active particles. We now consider the motion of active particle in viscosity gradients. We first look at the case where viscosity variations are due to the squirmer itself, in the spirit of [14] where the viscosity field varies radially due to the temperature of the particle, one may choose a viscosity field as shown in (9) where r is measured from the origin at the centre of the squirmer to find that the translational velocity of the squirmer is given by

$$\mathbf{U} = \frac{2B_1}{3} \left(1 - \frac{\varepsilon}{12}\right) \mathbf{e}, \quad (10)$$

where \mathbf{e} is the orientation of the squirmer. This indicates that a squirmer swimming in a region of radially increasing viscosity around it swims slower than in a Newtonian fluid with uniform viscosity. This can be understood by decomposing the swimming problem into a thrust problem and a drag problem [20]. In the thrust problem, the squirmer is held fixed and the thrust due to its surface velocity is calculated. In the drag problem, the drag on a passive sphere translating with the velocity of the squirmer is calculated. Such a decomposition shows that the viscosity gradient leads to reduction in both the

thrust and the drag, but the change in the thrust is more pronounced than the drag leading to slower swimming much like one observes in a shear-thinning fluid [20]. The angular velocity of the squirmer is zero in this case because of the symmetry of the problem.

Exact expressions for the translational and angular velocities of general squirmers can be obtained from (2) in linear viscosity fields such as (1). These are, up to $\mathcal{O}(\varepsilon)$,

$$\mathbf{U} = \mathbf{U}_N - \frac{aB_2}{5} (\mathbf{I} - 3\mathbf{e}\mathbf{e}) \cdot \nabla(\eta/\eta_0), \quad (11)$$

$$\mathbf{\Omega} = -\frac{1}{2} \mathbf{U}_N \times \nabla(\eta/\eta_0), \quad (12)$$

where $\mathbf{U}_N = (2B_1/3) \mathbf{e}$ is the velocity in a (Newtonian) fluid with uniform viscosity ($\mathbf{\Omega}_N = \mathbf{0}$). Note that the gradient in viscosity affects both the angular and translational velocities of the squirmer; even an axisymmetric squirmer can now rotate due to its own motion, in contrast, to a fluid with constant viscosity. The rotation of the squirmer is driven by the motion of the squirmer and is in the opposite sense to that of a passive sphere dragged along the same direction (see (8)). Equation (11) suggests that even with $\mathbf{U}_N = \mathbf{0}$, the squirmer may swim. That symmetric squirming modes may contribute to the swimming speed was also noted by Eastham and Shoele [16] for squirmers moving in fluids in which the viscosity is a function of the concentration of surrounding nutrients.

From equations (11) and (12), we note that if the swimmer moves along the gradient, $\mathbf{e} \parallel \nabla\eta$, it does not rotate ($\mathbf{\Omega} = \mathbf{0}$), and therefore maintains its original orientation. If we write $\nabla\eta = \beta\mathbf{e}$ then $\mathbf{U} = (1 + (3\alpha/5)\beta a/\eta_0) \mathbf{U}_N$. Depending on its type of propulsion, and consequently, on the sign of $\alpha = B_2/B_1$, it can swim faster, slower or at the same speed as in a Newtonian fluid with uniform viscosity. When the particle swims down a viscosity gradient, $\beta < 0$, puller swimmers ($\alpha < 0$) swim faster, because they generate thrust (or pull) at the front which is in a fluid more viscous than that in the back. Pushers ($\alpha > 0$), on the contrary, swim slower as they push on the less viscous fluid at their rear. Neutral swimmers ($\alpha = 0$), which have drag and thrust centres that coincide, swim with the Newtonian speed. The dynamics for pullers and pushers reverses when swimming up a viscosity gradient $\beta > 0$. When the swimming trajectory is not parallel to the viscosity gradient the orthogonal component will induce an out-of-plane rotation on the swimmer and can also cause drift velocity along the gradient. For example, if we take the $\nabla\eta = \beta_\perp \mathbf{e}_\perp$ where $\mathbf{e} \cdot \mathbf{e}_\perp = 0$ we obtain $\mathbf{U} = \mathbf{U}_N - (aB_2/5\eta_0) \beta_\perp \mathbf{e}_\perp$ and $\mathbf{\Omega} = -(\eta_0/2) \mathbf{U}_N \times \beta_\perp \mathbf{e}_\perp$. Note that the drift along the viscosity gradient depends only on the second squirming mode B_2 , which governs whether fluid is drawn into ($B_2 < 0$) or expelled from ($B_2 > 0$) around the equator of the swimmer and causes drift up or down the gradient respectively; this motion may arise even when $\mathbf{U}_N = \mathbf{0}$. The general case is simply

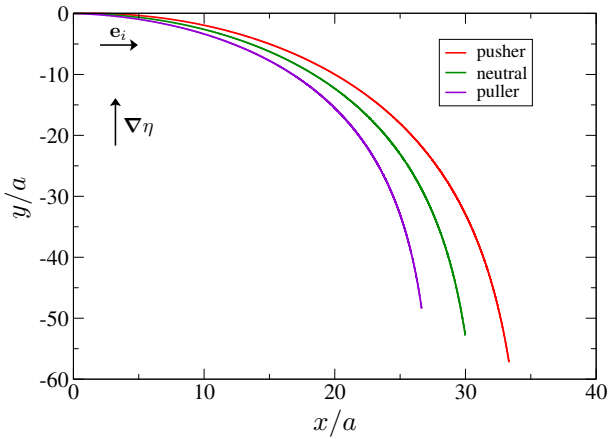


FIG. 1. The initial orientation of the swimmers \mathbf{e}_i is along the positive x-axis. The viscosity gradient is along the positive y-axis. After sometime all swimmers swim antiparallel to the viscosity gradient. Note that in this orientation, pushers are the fastest, while pullers are the slowest. The trajectories are plotted for time $t = 0$ to $t = 100a/B_1$.

a linear superposition of these cases.

These results can all be understood by examining the effect of the viscosity gradient on thrust and drag separately. One finds that for a squirmer, the change in thrust is opposite to the change in drag and dominant in magnitude, consequently, the squirmer rotates in a direction opposite to that of a passive sphere (one can picture for example a small row boat in a viscosity gradient, where the differences in the viscosity between the paddles dominates the change in dynamics). Also note that of all squirmering modes B_l , only the first two contribute to the translational and rotational velocities in the linear gradients considered here.

In general, when the swimming direction is not perfectly aligned with the viscosity gradient, irrespective of the type of propulsion, squirmers rotate toward the direction of lower viscosity and hence display viscoprobicity (negative viscotaxis). We demonstrate this in figure 1, where we consider the motion of squirmers in the plane of the viscosity gradient. We take $\nabla\eta$ parallel to \mathbf{e}_y and the initial orientation of swimmers along \mathbf{e}_x , as shown in figure 1. We take $\alpha = 0$ for neutral squirmers, and $\alpha = 2$ and $\alpha = -2$ for pullers and pushers, respectively, and set $\varepsilon = 0.1$. As we can see in figure 1, the final equilibrium orientation for all the swimmers is down the viscosity gradient; however, the trajectories do depend on the type of swimmer. Pushers swim furthest, both laterally across the gradient and vertically along the gradient, pullers remain the nearest. These differences in trajectories could then be used to sort the swimmers, for example, based on distance perpendicular to the gradient, from the point of release.

For the same values of α and ε , we also plot trajectories of squirmers (in this case, with only the first two squirm-

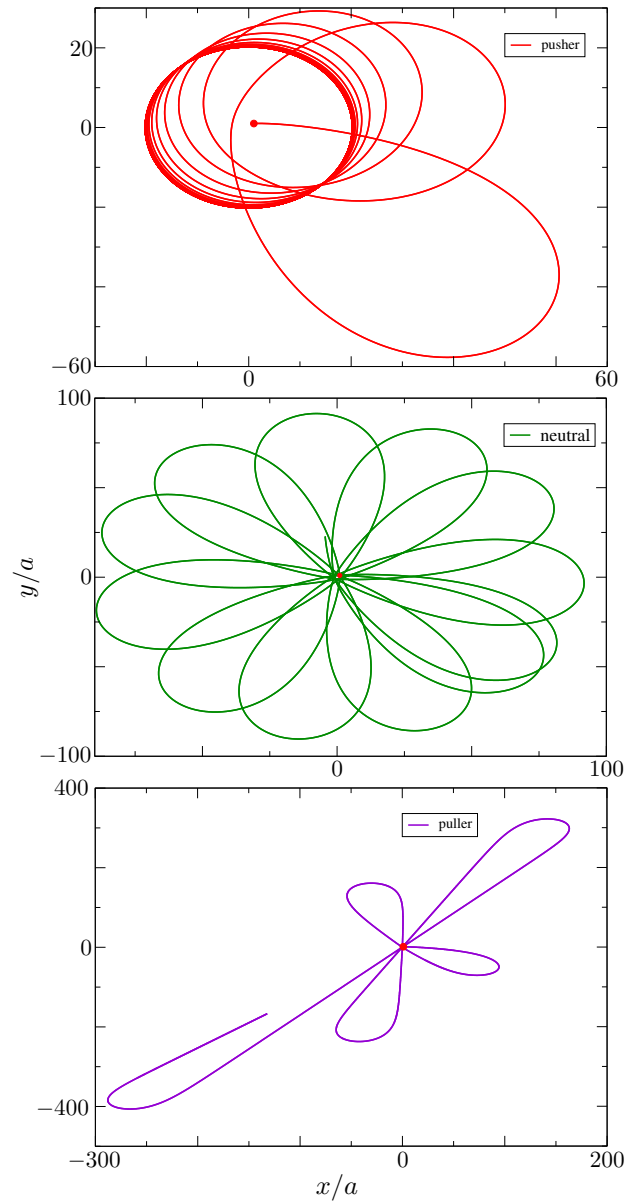


FIG. 2. Planar trajectories of pushers (left), neutral swimmers (centre), and pullers (right). The initial position of the swimmers, $(x/a = 1, y/a = 1)$, is marked by the red dot. The swimmers originally point in the positive x-axis. The swimmers are in a radial viscosity gradient: viscosity increases radially outward from the origin. All trajectories run until $t = 4000a/B_1$.

ing modes) moving in a plane with a radially varying two-dimensional viscosity field of the form $\nabla\eta = (\eta_0/R)\mathbf{e}_r$ where \mathbf{e}_r is the in-plane radial direction in cylindrical coordinates, and the origin in the coordinate system is defined at an arbitrary point in the fluid which may be seen as a ‘viscosity sink’. Here $\varepsilon = a/R \ll 1$ and $\eta_1 = \eta_0 r/a$ where $r^2 = x^2 + y^2$. We use a locally linear approximation whereby the local dynamics are given by (11) and (12) to calculate the trajectories. Although the expressions have

been derived only for linear gradients, they are expected to hold for radial gradients as well, for at the scale of the particle, little difference should exist between the two due to small curvatures (except at the origin). The trajectories are plotted in figure 2. In particular, one should note the qualitatively different behaviour of the three types of swimmers. Pushers find a stable orbit about the ‘origin’ of viscosity gradient, the trajectory of neutral swimmers is bounded at long times but in contrast, trajectories of pullers grows unbounded.

In order to analyze the two-dimensional motion of squirmers in the planar radial gradient mentioned above the orientation vector \mathbf{e} represented as $\{\cos \theta, \sin \theta\}$, and the gradient viscosity as $\nabla(\eta/\eta_0) = \varepsilon \{\cos \omega, \sin \omega\}/a$, where θ and ω are measured from the x-axis. Equations (11) and (12) then become

$$\frac{a}{B_1} \frac{d\psi}{dt} = \frac{1}{3} \varepsilon \sin \psi - \frac{a}{r} \left(\frac{2}{3} \sin \psi + \frac{3}{10} \varepsilon \alpha \sin 2\psi \right), \quad (13)$$

$$\frac{1}{B_1} \frac{dr}{dt} = \frac{2}{3} \cos \psi + \frac{3}{5} \varepsilon \alpha \left(\frac{2}{3} - \sin^2 \psi \right), \quad (14)$$

where $\psi = \theta - \omega$. The fixed points, when $\dot{\psi} = 0$, $\dot{r} = 0$, are $r_0/a = \frac{1}{\varepsilon} \left(2 + \frac{9}{5} \varepsilon \alpha \cos \psi_0 \right)$ $\psi_0 = \cos^{-1} \left[-(5/9\varepsilon\alpha) \left(1 \pm \sqrt{1 + (27/25)\varepsilon^2\alpha^2} \right) \right]$ for $\alpha \neq 0$. When $\alpha = 0$, we have $\psi_0 = \pi/2$ and $r_0/a = 2/\varepsilon$. With $\varepsilon = 0.1$, for $\alpha = \pm 2$ (values for pusher and pullers), we obtain $r_0/a = 20.21$ and $\psi_0 = 1.5114$. For neutral swimmers, $\alpha = 0$, $r_0/a = 20$ and $\psi_0 = \pi/2$.

We find that for pushers, the fixed point is a stable spiral, while for pullers, it is an unstable spiral. For neutral swimmers, the fixed point is a centre. These characteristics can be readily observed in figure 2. For such a simple gradient, we observe very different dynamics of the three types of squirmers. In radial gradients, neutral and pusher swimmers will remain bounded / trapped near the viscosity ‘sink’. The puller swimmers can therefore be sorted out at farther distances.

In summary, we observe that axisymmetric squirmers are, in general, viscopophobic. Unless they are perfectly aligned with the gradient, they turn towards regions of less viscosity. This is in contrast to the work of Liebchen *et al.* [15] who found no viscotaxis for uniaxial swimmers. Using the squirmer model, we find that the effects of viscosity gradients on the dynamics of active particles depend on their propulsion type and even simple viscosity fields lead to different dynamics for different microswimmers. The change in the dynamics of the swimmers can be readily explained by separately investigating the change in thrust and drag; while viscosity gradients affect both the drag on the body and the thrust generated by the swimming gait, the change in the latter tends to dominate the response. Finally, we showed that the differences in the dynamics due to swimming in viscosity gradients can be used to sort these swimmers by carefully choosing the viscosity profile.

The authors gratefully acknowledge funding from the Natural Sciences and Engineering Research Council of Canada (NSERC).

* Electronic mail: gelfring@mech.ubc.ca

- [1] J. N. Wilking, T. E. Angelini, A. Seminara, M. P. Brenner, and D. A. Weitz, *MRS Bulletin* **36**, 385 (2011).
- [2] A. Swidsinski, B. C. Sydora, Y. Doerffel, V. Loening-Baucke, M. Vaneechoutte, M. Lupicki, J. Scholze, H. Lochs, and L. A. Dieleman, *Inflamm. Bowel Dis.* **13**, 963 (2007).
- [3] R. R. Bennett and R. Golestanian, *J. R. Soc. Interface* **12**, 20141164 (2015).
- [4] H. C. Berg and D. A. Brown, *Nature* **239**, 500 (1972).
- [5] N. Waisbord, C. T. Lefevre, L. Bocquet, C. Ybert, and C. Cottin-Bizonne, *Phys. Rev. Fluids* **1**, 053203 (2016).
- [6] A. Bahat, I. Tur-Kaspa, A. Gakamsky, L. C. Giojalas, H. Breitbart, and M. Eisenbach, *Nat. Med.* **9**, 149 (2003).
- [7] A. M. Roberts, *J. Exp. Biol.* **213**, 4158 (2010).
- [8] K. Takabe, H. Tahara, M. S. Islam, S. Affroze, S. Kudo, and S. Nakamura, *Microbiology* **163**, 153 (2017).
- [9] M. J. Daniels, J. M. Longland, and J. Gilbert, *Microbiology* **118**, 429 (1980).
- [10] M. Y. Sherman, E. Timkina, and A. Glagolev, *FEMS Microbiol. Lett.* **13**, 137 (1982).
- [11] M. G. Petrino and R. N. Doetsch, *Microbiology* **109**, 113 (1978).
- [12] H. Yoshioka, Y. Sato, S. Yoshida, S. Ohtsubo, *et al.*, “Hydrogel for cell separation and method of separating cells,” (2006), US Patent App. 10/545,935.
- [13] M. Laumann and W. Zimmermann, *arXiv preprint arXiv:1903.11018* (2019).
- [14] N. Oppenheimer, S. Navardi, and H. A. Stone, *Phys. Rev. Fluids* **1**, 014001 (2016).
- [15] B. Liebchen, P. Monderkamp, B. ten Hagen, and H. Löwen, *Phys. Rev. Lett.* **120**, 208002 (2018).
- [16] P. S. Eastham and K. Shoele, *arXiv preprint arXiv:1904.01946* (2019).
- [17] M. J. Lighthill, *Commun. Pure Appl. Math.* **5**, 109 (1952).
- [18] J. R. Blake, *J. Fluid Mech.* **46**, 199 (1971).
- [19] T. J. Pedley, *IMA J. Appl. Math.* **81**, 488 (2016).
- [20] C. Datt, L. Zhu, G. J. Elfring, and O. S. Pak, *J. Fluid Mech.* **784**, R1 (2015).
- [21] C. Datt, G. Natale, S. G. Hatzikiriakos, and G. J. Elfring, *J. Fluid Mech.* **823**, 675 (2017).
- [22] E. Lauga, *Europhys. Lett.* **86**, 64001 (2009).
- [23] L. Zhu, E. Lauga, and L. Brandt, *Phys. Fluids* **24**, 051902 (2012).
- [24] M. De Corato and G. D’Avino, *Soft Matt.* **13**, 196 (2017).
- [25] G. J. Li, A. Karimi, and A. M. Ardekani, *Rheol. Acta* **53**, 911 (2014).
- [26] T. Ishikawa, M. P. Simmonds, and T. J. Pedley, *J. Fluid Mech.* **568**, 119 (2006).
- [27] O. S. Pak and E. Lauga, *J. Engng. Math.* **88**, 1 (2014).
- [28] G. J. Elfring, *J. Fluid Mech.* **829**, R3 (2017).
- [29] C. Datt and G. J. Elfring, *J. Non-Newton. Fluid Mech.* **262**, 107 (2018).
- [30] W. Yan and J. F. Brady, *Soft Matter* **11**, 6235 (2015).